Tissue hypoxia correlates with intensity of interictal spikes

Andrew S Geneslaw, Mingrui Zhao, Hongtao Ma and Theodore H Schwartz

Department of Neurological Surgery, Weill Medical College of Cornell University, New York Presbyterian Hospital, New York, New York, USA

Interictal spikes (IISs) represent burst firing of a small focal population of hypersynchronous, hyperexcitable cells. Whether cerebral blood flow (CBF) is adequate to meet the metabolic demands of this dramatic increase in membrane excitability is unknown. Positron emission tomography, single photon emission computed tomography, and functional magnetic resonance imaging studies have shown increases in CBF and hypometabolism, thus indicating the likelihood of adequate perfusion. We measured tissue oxygenation and CBF in a rat model of IIS using oxygen electrodes and laser-Doppler flowmetry. A $\sim$3-second dip in tissue oxygenation was shown, followed by more prolonged tissue hyperoxygenation, in spite of a 25% increase in CBF. Increases in the number of spikes, as well as in their amplitude and spike width further amplified these responses, and a decrease in interspike interval decreased the CBF response. Altering the anesthetic did not influence our results. Taken together, these findings indicate that frequent, high-amplitude IISs may produce significant tissue hypoxia, which has implications for patients with epilepsy and noninvasive techniques of seizure localization.

Introduction

Seizure localization using hemodynamic surrogates of neuronal activity measured with noninvasive imaging techniques such as single photon emission computed tomography, electroencephalogram-triggered functional magnetic resonance imaging (fMRI), and near-infrared spectroscopy are becoming more common in the work-up of patients with medically intractable epilepsy (Roche-Labarbe *et al*, 2008; Salek-Haddadi *et al*, 2006; Spencer, 1994). Interpretation of the resulting data relies on an understanding of the unique neurovascular coupling mechanisms that exist during epileptic events, which is not completely understood. Although these techniques can record both interictal and ictal activities, in practice, interictal events are more commonly recorded based on their higher frequency and the relatively slow hemodynamic response function, which often blurs the actual onset site of ictal events (de Curtis and Avanzini, 2001).

Recent studies have shown that interictal spikes (IISs) elicit a consistent, focal increase in cerebral blood flow (CBF) and cerebral blood volume (CBV) as small-caliber vessels dilate, bringing oxygenated blood to the pool of activated neurons (Hirase *et al*, 2004; Ma *et al*, 2009*b*; Suh *et al*, 2005; Vanzetta *et al*, 2010). However, the temporal delay in vascular dilatation raises the possibility that the metabolic demand of neurons may transiently overwhelm the supply of oxygen causing a temporary decrease in tissue oxygenation. This phenomenon, known as the 'initial dip' has been shown during normal physiologic processing using optical recording of intrinsic signals (ORISs) (Frostig *et al*, 1990), fMRI (Kim *et al*, 2000; Logothetis *et al*, 1999), and direct measurements with oxygen electrodes (Thompson *et al*, 2003). Whether a similar phenomenon occurs during IISs is not clear, although ORIS data support the existence of an early decrease in hemoglobin oxygenation, labeled the 'epileptic dip' (Bahar *et al*, 2006; Ma *et al*, 2009*b*; Suh *et al*, 2005). Unfortunately, the translation of ORIS data, which records relative changes in total and oxygenated hemoglobin using various wavelengths of light, into quantifiable hemodynamic responses is not straightforward, and early increases in CBV may be misinterpreted as initial decreases in hemoglobin oxygenation (Sirotin and Das, 2009). In addition, it has long been known that positron emission tomography (PET) imaging of

the interictal state shows hypometabolism, consistent with a net decrease in neuronal activity (Engel *et al*, 1990). This finding is difficult to reconcile with the increase in metabolism required to elicit a decrease in hemoglobin oxygenation, although the temporal resolution of PET is poor and may reflect metabolic activity occurring between IISs or neuronal loss in the epileptic focus. For this reason, we directly measured both CBF and tissue oxygenation using an oxygen-sensitive microelectrode in an animal model of IIS. We report a clear early dip in tissue oxygenation associated with each IIS, in spite of a large increase in CBF and characterize the dependence of tissue oxygenation and hemodynamic response on IIS amplitude, width, and frequency.

Materials and methods

Animal Preparation

All experimental procedures were approved by the Weill Cornell Medical College Animal Care and Use Committee following NIH (National Institutes of Health) guidelines. Adult male Sprague–Dawley rats ($n = 10$, weight = 250 to 380 g) were initially anesthetized with a mixture of 2% to 4% isoflurane in 70% N_2:30% O_2 by facemask, and maintained on 1% to 3% isoflurane in 70% N_2:30% O_2. Body temperature, heart rate, arterial blood oxygen saturation, and end-tidal CO_2 were carefully monitored and maintained stable at normal values as described previously (Zhao *et al*, 2009). The skull was thinned, and a small hole (1 mm²) was made in the skull and dura above the somatosensory cortex. An additional set of experiments was performed using urethane anesthesia (1.25 g/kg) (see Supplementary Materials).

Electrophysiology

A single-barreled glass microelectrode (impedance, 2 to 4 MΩ) filled with 0.9% saline for local field potential (LFP) recording was advanced into layers II to III of the cortex ($\sim 300 \mu$m). The LFP was amplified and filtered between 0.1 and 500 Hz using a DAB-S system (World Precision Instruments, Sarasota, FL, USA), and digitized at 1,000 Hz using CED Power 1401 (Cambridge Electronic Design, Cambridge, UK). Data including LFP, laser-Doppler flowmetry (LDF), and tissue oxygenation were recorded by a personal computer running the Spike2 software (Cambridge Electronic Design).

A second glass pipette (tip resistance 4 to 6 MΩ) was filled with a solution of bicuculline methiodide (BMI) (5 mmol/L in 165 mmol/L NaCl, pH 3.0; Sigma-Aldrich, St Louis, MO, USA) and positioned <1 mm from the LFP electrode. Iontophoresis of BMI was induced using a dual current generator (World Precision Technology, Sarasota, FL, USA). Currents ranged from −15 to −20 nA for retention and from +50 to +800 nA for release, depending on the resistance of the micropipette tip. Positive currents were maintained at 800 nA until stereotypical IISs were recorded. From this point on, positive current was manipulated within the stated range to keep IIS frequency between 0.2 and 5 Hz.

Tissue Oxygen Measurements

In the first set of experiments ($n = 5$ animals), a Clarke-style tissue-oxygen microelectrode (Unisense A/S, Aarhus N, Denmark) was used to measure cortical oxygen response to IISs. The O_2 electrode was calibrated in saline for a minimum of 2 hours at 37°C, first in atmospheric gas and then with pure nitrogen gas, to establish minimum and maximum oxygenation levels and a linear signal response curve. The 90% response time of these electrodes was 0.5 seconds. The O_2 electrode was then inserted to the same cortical depth as the BMI and LFP electrodes, as near to the BMI electrode as possible, typically < 100 μm. The signal was measured using a high-impedance picoammeter (PA 2000, Unisense A/S), digitized at 20 Hz.

Cerebral Blood Flow

In the second set of experiments ($n = 5$ animals), an LDF probe (wavelength, 780 nm; fiber separation, 0.25 μm, Perimed AB, Stockholm, Sweden) was used to measure the CBF response to IISs. Laser-Doppler flowmetry provides continuous hemodynamic monitoring of red blood cell velocity and red cell concentration, yielding a calculated CBF measure that correlates with traditional methods (Skarphedinsson *et al*, 1988). The LDF probe was placed just over the cortical surface, as close as possible to the BMI electrode (< 100 μm). Laser-Doppler flowmetry probes were recalibrated before each experiment. Laser-Doppler flowmetry measurements were continuously recorded using the PeriFlux System 5000 (Perimed AB).

Data Analysis

Data were analyzed offline using functions packaged with Spike2 software, and using custom-written software in Matlab (The Mathworks, Natick, MA, USA). An automated spike-detection algorithm was developed to tag times at which an IIS occurred in the LFP recording. The LFP was tagged as an IIS if the recording was ± 2 s.d. from the mean for that animal, and if the LFP had not exceeded that threshold for at least 10 milliseconds before. Once the entire LFP recording had been tagged for each IIS, any IIS segment occurring within 1 second of each other was grouped together as 'polyspikes.' Before the onset of each single or poly IIS, at least 5 seconds of clean LFP recording without an IIS was required, ensuring that local CBF and metabolism had enough

time to return to baseline. Interictal spikes lacking this preceding spike-free duration were excluded from the data set.

We separated each IIS into 3 separate categories based on the number of spikes within 2 seconds of spike onset: 1 spike (n_1), 2 spikes (n_2), and $\geqslant 3$ spikes (n_3). Interictal spikes with additional spikes after the initial 2 seconds were also excluded from the data set so that we could analyze the hemodynamic response for a period of time without contamination from other IIS events.

Amplitude of Hemodynamic Changes

Both pO_2 and LDF recordings were applied an offline Chebyshev Type II low-pass filter to remove heartbeat and breathing artifact. The pO_2 and LDF baselines were determined as the mean value during the 100 milliseconds before the onset of each IIS. Local changes in pO_2 and CBF were thus measured as the percentage change from the immediately preceding baseline mean. Maxima and minima were recorded for both pO_2 and LDF changes, and data were averaged within groups based on the number of IISs (n_1, n_2, or n_3). These average values were then compared both with each other, and also with the other recorded signal modalities (such as CBF increase, pO_2 decrease, etc.) using one-way analysis of variance (ANOVA), followed by multiple t-tests for significance, or two-way t-tests in comparisons between only two variables. The Bonferroni method was used to correct significance levels whenever multiple comparisons were used. The quantitative correlation between LFP variables such as amplitude and width and changes of pO_2 or CBF was determined by computing the Spearman correlation coefficient.

Onset and Duration of Hemodynamic Changes

We calculated the onset and offset of hemodynamic changes using a threshold value of baseline ± 2.5 s.d. Once marked according to these criteria, the onset and duration of changes were compared similarly as discussed above, using one-way ANOVA with multiple t-tests, or two-way t-tests. All data were expressed as mean $\pm$ s.e.m.

Results

Interictal spikes were successfully recorded from 10 animals, with an average spike frequency of 0.46 ± 0.35 Hz. A total of 978 IISs matching our selection criteria were recorded, 480 with concurrent LDF and 498 with pO_2 measurements (Figures 1A and 1B).

The LDF response consisted of a monophasic increase in CBF, with the mean latency of 0.65 ± 0.53 seconds (Figure 1C). The mean duration

of LDF increase was 6.12 ± 2.22 seconds. The maximum amplitude of LDF increase was $27.76\% \pm 5.57\%$, occurring 2.0 ± 0.63 seconds after the IIS (Figure 1D). In 251 out of 478 IISs, the increase in LDF did not return to baseline within the 8-second duration of the recording.

Tissue oxygenation showed a biphasic response to each IIS, consisting of an initial dip in pO_2, followed by a period of hyperoxygenation (Figure 1C). Tissue pO_2 began to decrease 0.79 ± 0.84 seconds after the first IIS, and remained below threshold for 2.66 ± 1.98 seconds. This decrease attained a minimum value of $-5.51\% \pm 2.52\%$ change from baseline at 1.57 ± 1.67 seconds. The pO_2 signal then inverted, continuing to increase until it exceeded the threshold at 3.02 ± 1.61 seconds. The pO_2 level remained elevated for 3.50 ± 2.13 seconds. The maximum amplitude attained was $6.98\% \pm 2.58\%$ change from baseline, at 3.09 ± 2.30 seconds (Figure 1D). Similar to the LDF recordings, 200 out of a total 406 recordings did not completely return to baseline within the 8-second duration of recording.

When compared by one-way ANOVA, amplitudes of the absolute values of pO_2 dip, pO_2 hyperoxygenation, and LDF increase were significantly different from one another, and *post hoc* tests indicated that the percentage increase in LDF was greater than both the dip in pO_2 and the subsequent hyperoxygenation, which were not significantly different from each other (Figure 1D). The two-sample t-test comparing the onset of changes in LDF and pO_2 showed that LDF changes began significantly earlier ($P < 0.01$).

Hemodynamic Response Based on the Number of Polyspikes

As a single IIS dramatically increases focal cerebral metabolism to supranormal levels, it was not clear how further increases in the degree of metabolic demand would impact the hemodynamic response. Iontophoresis of BMI often resulted in clusters of IISs in addition to single IISs. Clusters of polyspikes were categorized based on the number of spikes occurring in a 1-second window after the first spike (Figure 1; see the 'Materials and methods' section). Spike clusters were grouped into three categories depending on whether there was one spike (n_1), two spikes (n_2), or three or more spikes (n_{3+}) (Figure 2A). The number of examples of each category for the pO_2 and LDF experiments was pO_2: $n_1 = 224$, $n_2 = 262$, $n_3 = 112$ and LDF: $n_1 = 212$, $n_2 = 171$, $n_3 = 97$.

As the number of IISs increased, so did the amplitude the CBF response (Figure 2B, left). Maximal CBF responses for n_1, n_2, and n_3 were $18.30\% \pm 0.93\%$, $25.74\% \pm 1.04\%$, and $34.98\% \pm 1.38\%$, respectively. Compared with a single IIS, a double or triple IIS cause a 41% and a 91% increase in CBF. One-way ANOVA followed by multiple t-test comparisons showed that all values were
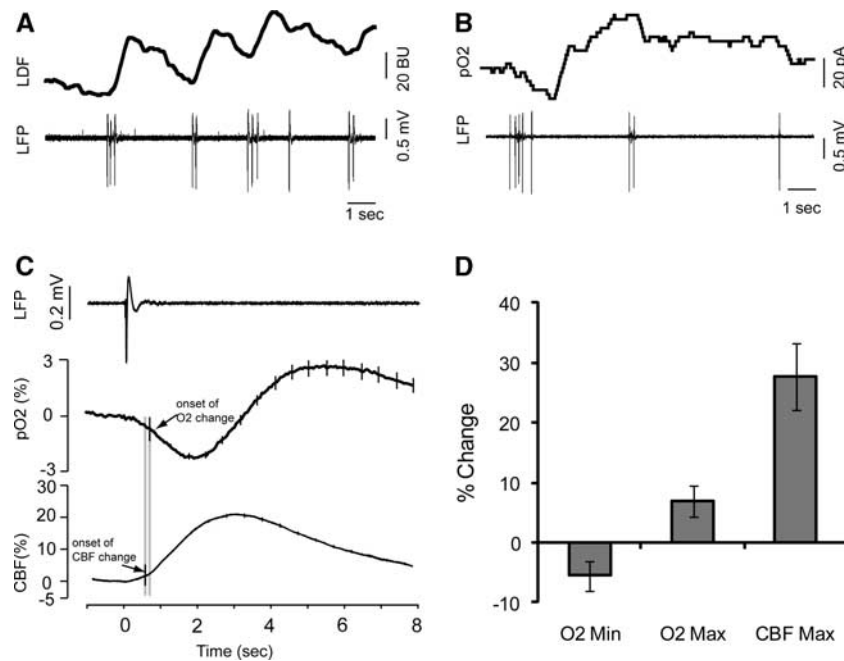
Figure 1 Example of the raw data before averaging. (**A**) LDF probe measures the increase in CBF (top panel) concurrently with LFP (bottom panel) measurements in a different animal. Increases in CBF can be clearly seen after each IIS event. (**B**) Polarographic pO_2-sensitive electrode measures tissue pO_2 (top panel) concurrently with LFP (bottom panel). A large dip in oxygenation and subsequent increase can be seen in response to the first cluster of 5 IISs. It must be noted that sometimes single IISs occur, whereas sometimes there are clusters of polyspikes. (**C**) Averaged LFP (top panel), O_2 (middle panel), and CBF (bottom panel) plots from all groups of spikes. Arrows indicate the onset of changes in each signal type based up thresholding as detailed in the 'Materials and methods' section. Error bars represent s.e. (**D**) Amplitude of average decrease and increase in O_2, and increase in CBF. Error bars show s.e. CBF, cerebral blood flow; IIS, interictal spike; LDF, laser-Doppler flowmetry; LFP, local field potential.

significantly different from each other ($F_{(1, 479)} = 51.62$, $P < 0.01$) (Figure 2C, left).

In spite of this increase in CBF, increases in the number of spikes also had a dramatic effect on the amplitude of the early dip in pO_2 (Figure 2B, right). The amplitude of the pO_2 dip increased from $-3.20\% \pm 0.34\%$ for n_1 to $-4.90\% \pm 0.40\%$ for n_2, and $-6.48\% \pm 4.8\%$ for n_3, each of which was significantly different from each other ($F_{(1, 497)} = 10.91$, $P < 0.01$). Compared with a single IIS, a double or triple IIS caused a 53% and a 103% increase in the amplitude of the early dip in O_2, which was larger than the percentage increase in the CBF response. As pO_2 changes were biphasic, we next analyzed the late hyperoxygenation phase of the recordings with regard to the number of spikes per IIS (Figure 2B, right). The average amplitude peaks of n_1, n_2, and n_3 were $3.23\% \pm 0.67\%$, $5.57\% \pm 0.79\%$, and $8.62\% \pm 0.95\%$, respectively. Analysis of variance found that the amplitudes of pO_2 increase were different for each group n_1, n_2, and n_3 ($F_{(1, 497)} = 1.66$, $P < 0.01$) (Figure 2C, right). Compared with a single IIS, double or triple IIS causes a 72% and a 167% increase in the amplitude of the delayed hyperoxygenation, which is a larger percentage change than either the CBF or early dip response. Similar results were obtained using urethane anesthesia (see Supplementary Materials).

Hemodynamic Response Based on Interictal Spike Amplitude and Width

In addition to the number of spikes, we attempted to correlate the hemodynamic response with the size of individual IISs. As the LFP is a measure mostly of subthreshold synaptic activity and partially of synchronized action potentials, the amplitude and width of each IIS reflect the size and duration of the population of neurons exhibiting a paroxysmal depolarization shift (PDS) and bursting, as well as the summed excitatory postsynaptic potentials of the involved neurons on the epileptic aggregate, which underlie the IIS. We hypothesized that IISs of different amplitudes and duration would elicit a variable hemodynamic response. We performed a correlation analysis to relate the maximum amplitude (LFP_{max}) and width (LFP_{width}) of the LFP response with the maximum amplitudes of the tissue pO_2 dip, hyperoxygenation, and the increase in CBF.

A Spearman correlation analysis showed a significant correlation between the LFP and the increases in CBF. For a total 480 LDF measurements, the amplitude of the CBF showed a strong significant correlation with LFP_{width} (Spearman's rank $r = 0.40$, $P < 0.0001$, Figure 3B). In addition, LFP_{max} correlated less well but still significantly with the amplitude of CBF ($r = 0.11$, $P < 0.02$, Figure 3A).
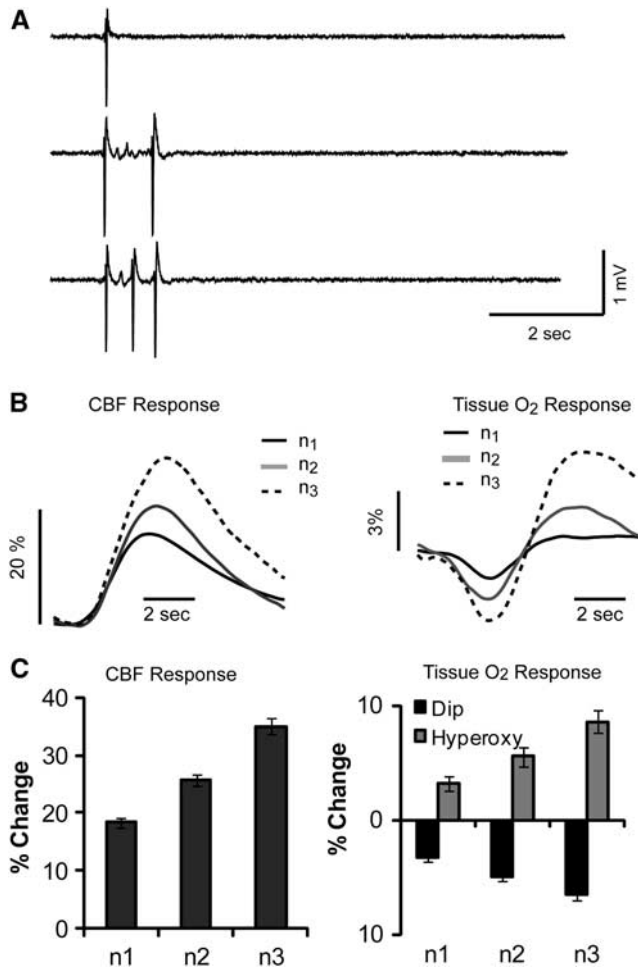
Figure 2 Hemodynamic responses to clusters of polyspikes. (**A**) Example of a single, double, and triple spike LFP recording. (**B**) Average values of CBF (left panel) and pO_2 (right panel) shows based on the number of spikes. (**C**) Maximum values increase for CBF (right panel), and for pO_2 increase and pO_2 decrease (left panel) are displayed as bar plots. Error bars show s.e. CBF, cerebral blood flow; LFP, local field potential.

For the total of 498 pO_2 measurements, the amplitude of the dip in tissue O_2 showed a significant negative correlation with both LFP_{max} ($r = -0.39$, $P < 0.0001$, Figure 3C) and LFP_{width} ($r = -0.19$, $P < 0.0001$, Figure 3D). A significant positive correlation was also found between the maximum amplitude of the hyperoxygenation response and LFP_{max} ($r = 0.14$, $P < 0.001$, Figure 3C), as well as LFP_{width} ($r = 0.40$, $P < 0.0001$, Figure 3D).

Relationship Between the Interspike Interval and Hemodynamic Response

As the hemodynamic response returns to baseline on a relatively slow timescale and an IIS can occur at frequencies with short interspike intervals before the hemodynamic response can return to its baseline, it is important to understand the impact of interspike interval on the hemodynamic response. All reported data thus far had a 5-second window in which no previous spikes occurred to eliminate the impact of previous spikes and residual hemodynamic response. We separately examined the hemodynamic response to single spikes that arose within 1, 2, 3, 4, or 5 seconds of a previous spike, i.e., increasing interspike interval. Although there was no significant change in either the pO_2 dip or the hyperoxygenation response, the increase in CBF, conversely, showed a significant increase as the interspike interval increased (one-way ANOVA with Bonferroni's corrected t-test, $P < 0.05$, Figure 3E).

Discussion

In this manuscript, for the first time, we unambiguously show a transient dip in tissue oxygenation after an IIS. This dip occurs in spite of a large $\sim 25\%$ increase in CBF, lasts for almost 3 seconds, and is followed by a larger, longer tissue hyperoxygenation. The dip in O_2 indicates that the increased metabolism of oxygen elicited by the IIS briefly overwhelms the ability of the brain to provide oxygenated blood by increasing CBF, thus causing a transient tissue hypoxia. We also found that the degree of dip, hyperoxygenation, and CBF increase correlates with the frequency, amplitude, and duration of each IIS, likely related to increases in metabolic demand. Although IISs elicited in this acute pharmacologic animal model may not be identical to those found in chronic human epilepsy, there is evidence for a similar process underlying human epileptic events, which may have a significant impact on our understanding of the role of IISs in human epilepsy and mechanisms for seizure localization.

Interictal Spikes

The IISs represent the synchronous paroxysmal firing of a small population of interconnected neurons that occurs between seizures in and around an epileptic focus (Schwartzkroin and Wyler, 1980). The cellular events underlying the IISs consist of a burst of action potentials, superimposed on a slow depolarizing potential, indicating a summation of excitatory synaptic potentials causing a dramatic increase in metabolic demand (Chamberlin et al, 1990). Although an increase in perfusion during epileptic events is universally shown in all previous studies, some find that perfusion oversupplied metabolism (Nersesyan et al, 2004; Tenney et al, 2004), whereas others show the opposite, namely inadequate perfusion to meet metabolic demand (Ingvar, 1986; Kreisman et al, 1991; Pereira de Vasconcelos et al, 2002; Tanaka et al, 1990). Investigators using interictal and ictal spike-triggered fMRI in humans generally report an increase in the blood oxygen-level dependent (BOLD) signal, which
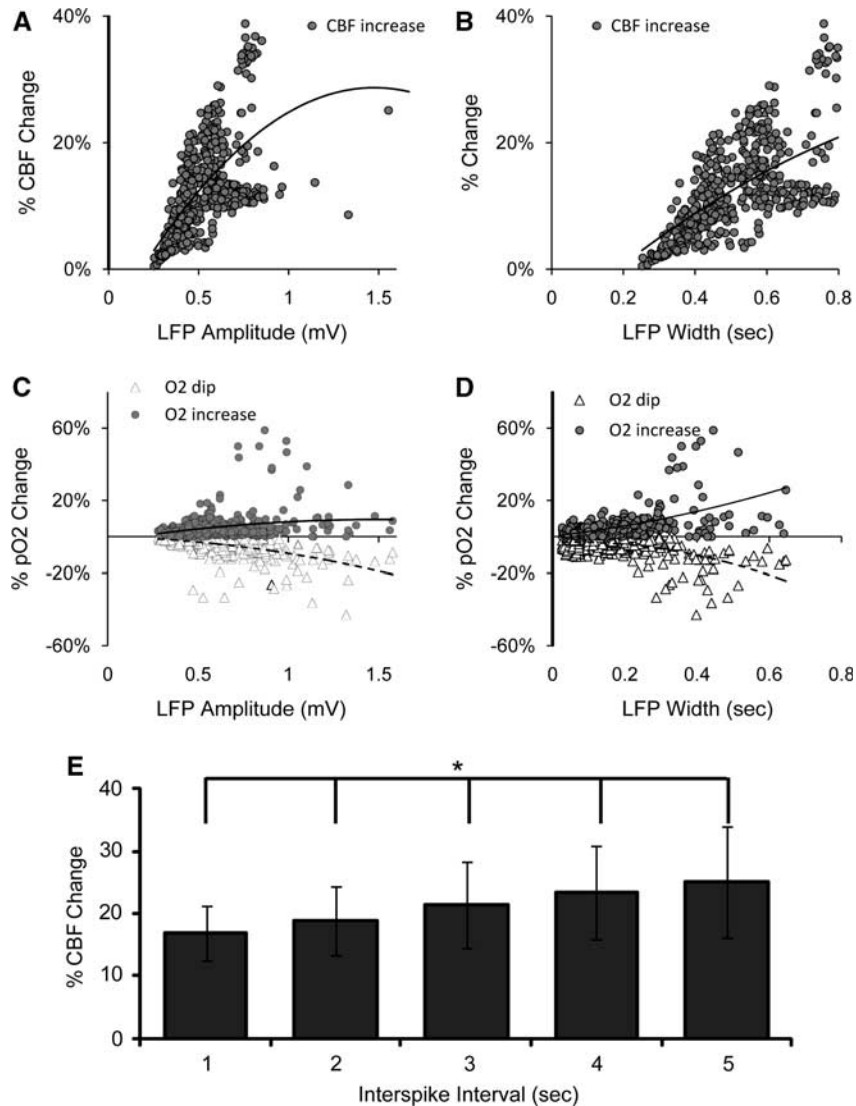
Figure 3 The relationship between the hemodynamic response and LFP$_{max}$, width and interspike interval. The CBF increase also significantly correlated with (**A**) LFP amplitude and (**B**) LFP width. (**C**) The LFP amplitude was correlated with oxygen dip and oxygen increases. (**D**) The LFP width was correlated with oxygen dip and oxygen increases. The trend line showed the positive or negative correlation. (**E**) CBF response shows a significant increase in amplitude as the interspike interval increases. *One-way ANOVA with *post hoc* Bonferroni's corrected *T*-tests, each significant from each other ($P < 0.05$). Error bars show s.e. ANOVA, analysis of variance; CBF, cerebral blood flow; LFP$_{max}$, maximum local field potential.

would be consistent with hyperoxygenation and adequate CBF (Salek-Haddadi *et al*, 2006). Similarly, interictal PET scans generally show hypometabolism, indicating that metabolic demand is not excessive during the interictal state, although the majority of this state is dominated by the interspike interval, and hence does not reflect metabolism from the spikes themselves and may also be a product of neuronal loss (Engel *et al*, 1990). In addition, the relationship between neuronal activity and metabolic demand is complex and inhibitory activity has been shown in some models, such as γ-oscillations, to have high metabolic demand, whereas action potentials may have minimal demands compared

with subthreshold synaptic activity (Alle *et al*, 2009; Kann *et al*, 2011).

In this study, a clear transient decrease in tissue oxygenation is shown, indicating that CBF is temporarily unable to meet the high metabolic demands of the IIS. However, between infrequent IISs, a period of longer-lasting hyperoxygenation ensues, elicited by the dramatic increase in CBF. Hence, CBF is more than adequate to meet metabolic demand if IISs are infrequent, but in a delayed manner. As anesthesia, particularly isoflurane can open the blood–brain barrier to increase CBF (Heinemann, 2008; Tétrault *et al*, 2008) and also activates pain receptors which can cause release of corticosteroids (Alexander *et al*,

2009; Matta *et al*, 2008), potentially influencing our results, we performed the same experiments under urethane anesthesia and results were similar, indicating that the anesthetic effect cannot explain our findings (see Supplementary Materials). It is also possible that our model, involving iontophoresis of GABA, may interfere with neurovascular coupling because studies have shown that GABA released by interneurons can directly dilate and constrict smooth muscle cells and may have a role in neurovascular coupling (Cauli *et al*, 2004; Rancillac *et al*, 2006). However, we have previously shown a similar effect in the 4-aminopyridine (4-AP) model and in spontaneous human epilepsy (Zhao *et al*, 2007, 2009).

We also show that increasing the number, amplitude, and width of IISs leads to a subsequent increase in the dip, hyperoxygenation, and CBF response as metabolic demand increases with further increases in excitatory synaptic activity. This finding is consistent with previous correlations between membrane potential and hemoglobin deoxygenation shown with voltage-sensitive dye imaging (Ma *et al*, 2009b) and animal PET studies, in which high-frequency IISs were shown to cause PET hypermetabolism (Bruehl *et al*, 1998). Furthermore, we show that with decreasing interspike interval, the CBF response also decreases, which further prolongs and amplifies tissue hypoxia. Taken together, these data indicate that patients with high-frequency IISs might have more prolonged periods of tissue hypoxia. Indeed, studies of transient cognitive impairment during IISs indicate that high frequency or longer duration of IISs are associated with a higher risk of transient cognitive impairment (Aldenkamp and Arends, 2004). The primary mechanism for this impairment is believed to be electrochemical, associated with a disruption in long-term potentiation, the synaptic mechanism underlying the formation of long-term memory (Moore *et al*, 1993). However, some authors raise the possibility of focal cerebral metabolic dysfunction as an etiology for transient cognitive impairment, based on interictal PET hypometabolism (Hughes *et al*, 1989). Our study raises another possible explanation for transient cognitive impairment, namely focal tissue hypoxia. Further human studies of this topic may be warranted.

Relevance to Human Epilepsy

Critics might argue that these animal studies have no bearing on human epilepsy. However, there is significant evidence to the contrary. Human studies of hemoglobin oxygenation during cortical stimulation and spontaneous seizures show decreases in hemoglobin oxygenation that mimic these animal studies, even in the absence of anesthesia (Suh *et al*, 2006; Zhao *et al*, 2007). Similarly, human studies during afterdischarges, which are subtended by similar cellular and network events as those under-

lying IISs, including the paroxysmal depolarizing shift (Ayala *et al*, 1973; Miles *et al*, 1984), also show transient decreases in hemoglobin oxygenation (Ma *et al*, 2009a). Functional magnetic resonance imaging studies also corroborate our data showing that the magnitude of the BOLD response is larger after a burst of spikes compared with a single spike and also correlates with spike amplitude (Al-Asmi *et al*, 2003; LeVan *et al*, 2010). Finally, direct tissue measurements of oxygen tension during seizures, performed almost 35 years ago, have also shown brief decreases in tissue oxygenation (Dymond and Crandall, 1976). Hence, although infrequent IISs, which may cause transient hypoxia have no clinically significant effect on cortical function, frequent longer-duration trains of IISs may be deleterious.

Significance for Imaging

Hemoglobin oxygenation during IISs has been investigated previously with ORIS (Ma *et al*, 2009b; Suh *et al*, 2005). These studies showed a brief ~3-second decrease in hemoglobin oxygenation at the onset of the IIS, similar but longer and higher in amplitude to the initial dip found in previous studies of normal cortical processing, which were confirmed with oxygen-sensitive electrodes (Ances *et al*, 2001; Thompson *et al*, 2003). However, Sirotin and Das (2009) recently showed that the so-called initial dip after normal cortical processing may be an artifact of an early focal increase in CBV, which calls into question the ORIS data on hemoglobin oxygenation during IISs. Our current study lays the question to rest, clearly showing a transient 'epileptic dip' in tissue oxygenation similar in length to the hemoglobin oxygenation dip shown with ORIS (Suh *et al*, 2005). However, we emphasize that these results are specific to the central region of the IIS, i.e., 'focus' and may not be true with increasing distance as one moves into the surround.

These data are important for researchers performing electroencephalogram-triggered fMRI because the BOLD signal arises both from the concentrations of oxygenated hemoglobin and CBV. The biphasic oxygen response and monophasic CBF response in our study highlight the temporal dependence of the directionality of the phenomenon underlying the BOLD signal. Functional magnetic resonance imaging laboratories will have to model these different responses in analyzing their data and may benefit from identifying an early negative BOLD signal, which may localize more precisely with the area of highest metabolism during an epileptic event (Buxton, 2010; Lin *et al*, 2010). Similarly, future technology that can image metabolism in the brain at higher spatial and temporal resolution than PET will likely provide extremely high-resolution localization of both the IIS and the ictal onset zone. Chronically implantable imaging devices currently under development that can measure CBV and blood

oxygenation during ictal onsets may also prove useful in the clinical setting (Cox *et al*, 2010).

Disclosure/conflict of interest

The authors declare no conflict of interest.

References

Al-Asmi A, Benar CG, Gross DW, Khani YA, Andermann F, Pike B, Dubeau F, Gotman J (2003) fMRI activation in continuous and spike-triggered EEG-fMRI studies of epileptic spikes. *Epilepsia* 44:1328–39

Aldenkamp A, Arends J (2004) The relative influence of epileptic EEG discharges, short nonconvulsive seizures, and type of epilepsy on cognitive function. *Epilepsia* 45:54–63

Alexander JK, DeVries AC, Kigerl KA, Dahlman JM, Popovich PG (2009) Stress exacerbates neuropathic pain via glucocorticoid and NMDA receptor activation. *Brain Behav Immun* 23:851–60

Alle H, Roth A, Geiger JRP (2009) Energy-efficient action potentials in hippocampal mossy fibers. *Science* 325:1405–8

Ances BM, Buerk DG, Greenberg JH, Detre JA (2001) Temporal dynamics of the partial pressure of brain tissue oxygen during functional forepaw stimulation in rats. *Neurosci Lett* 306:106–10

Ayala GF, Dichter M, Gumnit RJ, Matsumoto H, Spencer WA (1973) Genesis of epileptic interictal spikes. New knowledge of cortical feedback systems suggests a neurophysiological explanation of brief paroxysms. *Brain Res* 52:1–17

Bahar S, Suh M, Zhao M, Schwartz TH (2006) Intrinsic optical signal imaging of neocortical seizures: the 'epileptic dip'. *Neuroreport* 17:499–503

Bruehl C, Wagner U, Huston JP, Witte OW (1998) Thalamocortical circuits causing remote hypometabolism during focal interictal epilepsy. *Epilepsy Res* 32:379–87

Buxton R (2010) Interpreting oxygenation-based neuroimaging signals: the importance and the challenge of understanding brain oxygen metabolism. *Front Neuroenerg* 2:8

Cauli B, Tong X-K, Rancillac A, Serluca N, Lambolez B, Rossier J, Hamel E (2004) Cortical GABA interneurons in neurovascular coupling: relays for subcortical vasoactive pathways. *J Neurosci* 24:8940–9

Chamberlin NL, Traub RD, Dingledine R (1990) Role of EPSPs in initiation of spontaneous synchronized burst firing in rat hippocampal neurons bathed in high potassium. *J Neurophysiol* 64:1000–8

Cox MP, Hongtao M, Bahlke ME, Beck JH, Schwartz TH, Kymissis I (2010) LED-based optical device for chronic *in vivo* cerebral blood volume measurement. *IEEE Trans Electron Devices* 57:174–7

de Curtis M, Avanzini G (2001) Interictal spikes in focal epileptogenesis. *Prog Neurobiol* 63:541–67

Dymond AM, Crandall PH (1976) Oxygen availability and blood flow in the temporal lobes during spontaneous epileptic seizures in man. *Brain Res* 102:191–6

Engel J, Jr, Henry TR, Risinger MW, Mazziotta JC, Sutherling WW, Levesque MF, Phelps ME (1990) Presurgical evaluation for partial epilepsy: relative contributions of chronic depth-electrode recordings versus FDG-PET and scalp-sphenoidal ictal EEG. *Neurology* 40:1670–7

Frostig RD, Lieke EE, Ts'o DY, Grinvald A (1990) Cortical functional architecture and local coupling between neuronal activity and the microcirculation revealed by *in vivo* high-resolution optical imaging of intrinsic signals. *Proc Natl Acad Sci USA* 87:6082–6

Heinemann U (2008) New dangers of anesthesia: isoflurane induced opening of the blood–brain barrier (commentary on Tétrault *et al*). *Eur J Neurosci* 28:1329

Hirase H, Creso J, Buzsaki G (2004) Capillary level imaging of local cerebral blood flow in bicuculline-induced epileptic foci. *Neuroscience* 128:209–16

Hughes RL, Yonas H, Gur D, Latchaw R (1989) Cerebral blood flow determination within the first 8 hours of cerebral infarction using stable xenon-enhanced computed tomography. *Stroke* 20:754–60

Ingvar M (1986) Cerebral blood flow and metabolic rate during seizures. Relationship to epileptic brain damage. *Ann N Y Acad Sci* 462:194–206

Kann O, Huchzermeyer C, Kovács R, Wirtz S, Schuelke M (2011) Gamma oscillations in the hippocampus require high complex I gene expression and strong functional performance of mitochondria. *Brain* 134(pt 2):345–58

Kim DS, Duong TQ, Kim SG (2000) High-resolution mapping of iso-orientation columns by fMRI. *Nat Neurosci* 3:164–9

Kreisman NR, Magee JC, Brizzee BL (1991) Relative hypoperfusion in rat cerebral cortex during recurrent seizures. *J Cereb Blood Flow Metab* 11:77–87

LeVan P, Tyvaert L, Gotman J (2010) Modulation by EEG features of BOLD responses to interictal epileptiform discharges. *Neuroimage* 50:15–26

Lin A-L, Gao J-H, Duong TQ, Fox PT (2010) Functional neuroimaging: a physiological perspective. *Front Neuroenergetics* 2:5

Logothetis NK, Guggenberger H, Peled S, Pauls J (1999) Functional imaging of the monkey brain. *Nat Neurosci* 2:555–62

Ma H, Geneslaw A, Zhao M, Suh M, Perry C, Schwartz TH (2009a) The importance of latency in the focality of perfusion and oxygenation changes associated with triggered afterdischarges in human cortex. *J Cereb Blood Flow Metab* 29:1003–14

Ma H, Zhao M, Suh M, Schwartz TH (2009b) Hemodynamic surrogates for excitatory membrane potential change during interictal epileptiform events in rat neocortex. *J Neurophysiol* 101:2550–62

Matta JA, Cornett PM, Miyares RL, Abe K, Sahibzada N, Ahern GP (2008) General anesthetics activate a nociceptive ion channel to enhance pain and inflammation. *Proc Natl Acad Sci USA* 105:8784–9

Miles R, Wong RK, Traub RD (1984) Synchronized afterdischarges in the hippocampus: contribution of local synaptic interactions. *Neuroscience* 12:1179–89

Moore CI, Browning MD, Rose GM (1993) Hippocampal plasticity induced by primed burst, but not long-term potentiation, stimulation is impaired in area CA1 of aged Fischer 344 rats. *Hippocampus* 3:57–66

Nersesyan H, Herman P, Erdogan E, Hyder F, Blumenfeld H (2004) Relative changes in cerebral blood flow and neuronal activity in local microdomains during generalized seizures. *J Cereb Blood Flow Metab* 24:1057–68

Pereira de Vasconcelos A, Ferrandon A, Nehlig A (2002) Local cerebral blood flow during lithium-pilocarpine seizures in the developing and adult rat:role of coupling

between blood flow and metabolism in the genesis of neuronal damage. *J Cereb Blood Flow Metab* 22:196–205

Rancillac A, Rossier J, Guille M, Tong X-K, Geoffroy H, Amatore C, Arbault S, Hamel E, Cauli B (2006) Glutamatergic control of microvascular tone by distinct GABA neurons in the cerebellum. *J Neurosci* 26: 6997–7006

Roche-Labarbe N, Zaaimi B, Berquin P, Nehlig A, Grebe R, Wallois F (2008) NIRS-measured oxy- and deoxyhemoglobin changes associated with EEG spike-and-wave discharges in children. *Epilepsia* 49:1871–80

Salek-Haddadi A, Diehl B, Hamandi K, Merschhemke M, Liston A, Friston K, Duncan JS, Fish DR, Lemieux L (2006) Hemodynamic correlates of epileptiform discharges: an EEG-fMRI study of 63 patients with focal epilepsy. *Brain Res* 1088:148–66

Schwartzkroin PA, Wyler AR (1980) Mechanisms underlying epileptiform burst discharge. *Ann Neurol* 7:95–107

Sirotin YB, Das A (2009) Anticipatory haemodynamic signals in sensory cortex not predicted by local neuronal activity. *Nature* 457:475–9

Skarphedinsson JO, Harding H, Thoren P (1988) Repeated measurements of cerebral blood flow in rats. Comparisons between the hydrogen clearance method and laser Doppler flowmetry. *Acta Physiol Scand* 134:133–42

Spencer SS (1994) The relative contributions of MRI, SPECT, and PET imaging in epilepsy. *Epilepsia* 35(Suppl 6):S72–89

Suh M, Bahar S, Mehta AD, Schwartz TH (2005) Temporal dependence in uncoupling of blood volume and oxygenation during interictal epileptiform events in rat neocortex. *J Neurosci* 25:68–77

Suh M, Bahar S, Mehta AD, Schwartz TH (2006) Blood volume and hemoglobin oxygenation response following electrical stimulation of human cortex. *Neuroimage* 31:66–75

Tanaka S, Sako K, Tanaka T, Nishihara I, Yonemasu Y (1990) Uncoupling of local blood flow and metabolism in the hippocampal CA3 in kainic acid-induced limbic seizure status. *Neuroscience* 36:339–48

Tenney JR, Duong TQ, King JA, Ferris CF (2004) FMRI of brain activation in a genetic rat model of absence seizures. *Epilepsia* 45:576–82

Tétrault S, Chever O, Sik A, Amzica F (2008) Opening of the blood–brain barrier during isoflurane anaesthesia. *Eur J Neurosci* 28:1330–41

Thompson JK, Peterson MR, Freeman RD (2003) Single-neuron activity and tissue oxygenation in the cerebral cortex. *Science* 299:1070–2

Vanzetta I, Flynn C, Ivanov AI, Bernard C, Benar CG (2010) Investigation of linear coupling between single-event blood flow responses and interictal discharges in a model of experimental epilepsy. *J Neurophysiol* 103:3139–52

Zhao M, Ma H, Suh M, Schwartz TH (2009) Spatiotemporal dynamics of perfusion and oximetry during ictal discharges in the rat neocortex. *J Neurosci* 29:2814–23

Zhao M, Suh M, Ma H, Perry C, Geneslaw A, Schwartz TH (2007) Focal increases in perfusion and decreases in hemoglobin oxygenation precede seizure onset in spontaneous human epilepsy. *Epilepsia* 48:2059–67